Adhesion strength of silver thick-film conductors by solder-free test

Y. ENOKIDO, T. YAMAGUCHI
Department of Materials Science, Faculty of Science and Technology, Keio University, Yokohama, Japan

Adhesion of silver thick-film conductors to alumina substrates was studied by a solderless testing method, in which alumina substrates were bonded with a silver thick-film and pulled vertically under a constant strain rate to fracture. The fracture behaviour was studied on thick films prepared under different conditions, and the effect of microstructure on the adhesion strength was studied. A new parameter has been introduced for evaluating the resistance to crack propagation. Hence, microstructural requirements for high adhesion strength thick films have been proposed. The adhesion strength data of silver thick films have been best described by a log-normal distribution function.

1. Introduction

Thick-film conductors have been used in hybrid integrated circuits for more than a quarter of a century. The adhesion strength of thick-film conductors to the substrate has become an important problem with the down-sizing trend in electronic devices. Generally, the adhesion strength of thick-film conductors to the substrate is evaluated by the peel test method [1–5] or pull test method [6, 7]. Besides these test methods, a two-side pull test [8, 9], a nail head test [10], a single beam test [11] and a double cantilever beam method [12] were reported. All these test methods require soldering the thick film to a wire or a jig, which results in the formation of intermetallics from the metal elements in the thick film and the solder. It is known that these intermetallics affect the adhesion strength of the thick film [5]. In addition, the measured strength contains elastic effects of the solder, wire and jig. Therefore, the intrinsic adhesion strength cannot be obtained by these test methods. The effects of soldering on the adhesion strength can be evaluated from the difference between the adhesion strengths with and without soldering. Hence, we can measure the adhesion strength of thick films for practical applications precisely.

The adhesion strength of thick-film conductors to the substrate depends on the behaviour of glass, a bonding agent incorporated in silver thick films, as well as on the interaction between glass and substrate. However, there is no systematic study of the relationship between adhesion strength and microstructure. In this paper, we studied the relation between adhesion strength and microstructure in silver thick-film conductors. To avoid the effects of soldering, we developed a new method of adhesion strength test; two substrates were bonded with thick-film paste, and pulled vertically to the substrates until they separated. The load and the displacement of the substrates were recorded continuously. Parameters for characterizing the microstructure have been defined and correlated with fracture behaviour.

2. Experimental procedure

2.1. Preparation of specimens

Two silver powders, Ag-c (Metz Metallurgical) and Ag-f (Sumitomo Metal Mining) with average sizes of 0.5 and 0.05 μm, respectively, were used. Three glass frits, Glass A (ASF1340, Asahi Glass), Glass B (ASF1370) and Glass C (ASF1380), were used. They were lead borosilicate glasses with softening points of 505, 615, and 705 °C, respectively. The average sizes of all these frits were 2.0 μm. Some 5 wt % ethyl cellulose diethylenglycol monobutylether (butylcarbitol) solution was used as an organic vehicle. Substrates containing 94% alumina (T.K.N) with dimensions of $24 \times 48 \times 3.5$ mm were used.

Silver thick-film pastes were prepared by mixing silver powder, glass frit and organic vehicle. The silver powder/glass frit ratios were 95/5, 90/10, 80/20 and 60/40 in volume. The powder/organic vehicle ratio was 4/1 in weight. The silver thick-film paste was printed at the centre of the substrate three times through a 200 mesh stainless screen. The size of the thick-film pad was 2.0 mm in diameter. Two printed substrates were bonded as shown in Fig. 1 with the silver thick-film paste while it was still wet. This specimen was heated at 450 °C for 15 min in air to burn out the organic vehicle, and fired in air at 650, 750 and 850 °C for 10 min in a belt furnace (DZ13-4-T4. 4MN Denko). Thick films with various microstructures were prepared by combining material parameters and processing conditions listed in Table I.

2.2. Adhesion strength and displacement measurement

Fig. 2 shows the instrument, jigs and the specimen for adhesion and displacement measurements. A tensile test machine (SLS, Imada) was used to load the specimen. The upper substrate of the specimen was placed on the lower jig. The lower substrate was pushed

0022–2461

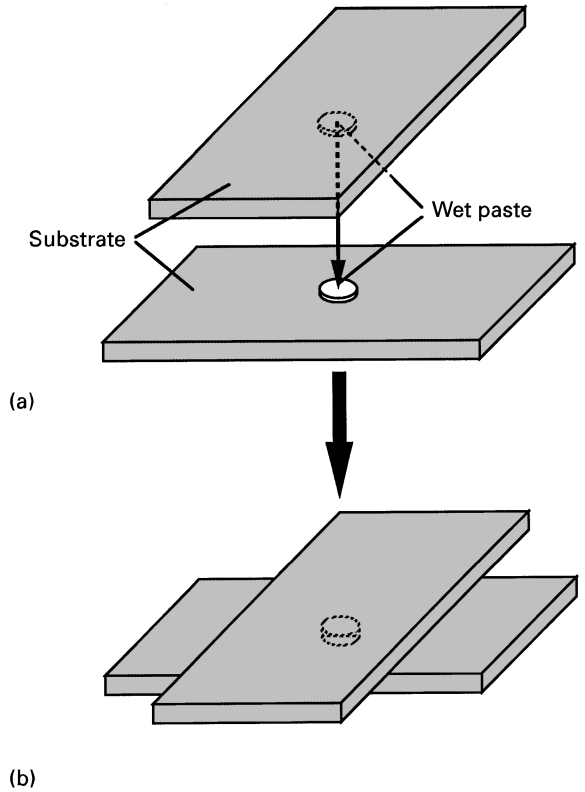

Figure 1 Specimen preparation: (a) before bonding with silver thick-film paste, and (b) after bonding.

TABLE I Preparation conditions of specimens[a]

Specimen	Silver	Glass	Volume of glass (%)	Firing temperture (°C)
Am7	Ag-c	A	20.0	750
Bm7	Ag-c	B	20.0	750
Cm7	Ag-c	C	20.0	750
Bm6	Ag-c	B	20.0	650
Bm8	Ag-c	B	20.0	850
Bll7	Ag-c	B	5.0	750
Bl7	Ag-c	B	10.0	750
Bh7	Ag-c	B	40.0	750
Bm7f	Ag-f	B	20.0	750

[a] A, B and C denote the glass composition, symbols h, m and l denote the glass contents; high, medium and low, respectively. The numerals 6, 7 and 8 stand for firing temperatures of 650, 750 and 850 °C, respectively.

down with the upper jig, which was connected to the tensile test machine through the digital force gauge (DPRS-50T, Imada). Then, the specimen was loaded at a crosshead speed of $15\,\mu m\,s^{-1}$ and the load was measured continuously. The displacement of the lower substrate of the specimen was measured with a linear gauge (LG-130, Mitsutoyo) and a linear gauge counter (LG-M1, Mitsutoyo). The linear guage was placed in contact with the upper surface of the lower jig. The digital force gauge and the linear gauge were connected to a personal computer through General Purpose Interface Bus (GP–IB) interfaces. Measured load and displacement were recorded continuously as a function of time. After the fracture of thick films, the diameter of the thick-film pad was measured with

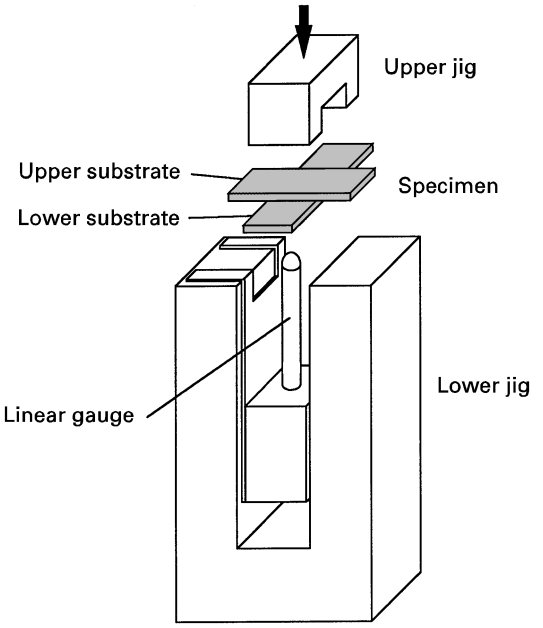

Figure 2 Instrument for measuring the adhesion strength and displacement.

a micrometer and the area of the pad was calculated. The strength was obtained by dividing the load by the area. The adhesion strength was calculated from 30 specimens prepared for each combination of material parameters under controlled temperature and humidity. Measured adhesion strengths were analysed by the Weibull, normal and log-normal distribution functions. Adhesion strengths were plotted on a probability paper, and correlation coefficients were calculated.

2.3. Microstructure observation

The fired specimens were cut vertically to the substrate with a diamond blade cutter and the cross-sections were polished with diamond slurries of 9, 3 and 1 μm. The polished specimens were etched in a mixture containing equal volumes of saturated NH_4OH and 3 vol% H_2O_2 aqueous solutions to observe grain boundaries. Backscattered electron images of specimens were observed with a scanning electron microscope (JSM-T100, Jeol).

3. Results and discussion

3.1. Strength–displacement curve

A typical strength–displacement curve is shown in Fig. 3. The gradient of the curve increased at around 3 MPa for all specimens, which resulted from plays of the jig and the digital force gauge, not from the displacement of the thick film. There are two characteristic points, designated as M and C. At point M, the gradient of the curve changes. About half of the specimens showed the gradient decrease at point M. A major fraction of the displacement was attributed to the warp of the upper substrate, as judged from the displacement–strength curve of a single substrate in a blank test. The displacement that originated from the warp of a substrate increased linearly in the measured strength range. Consequently, the gradient

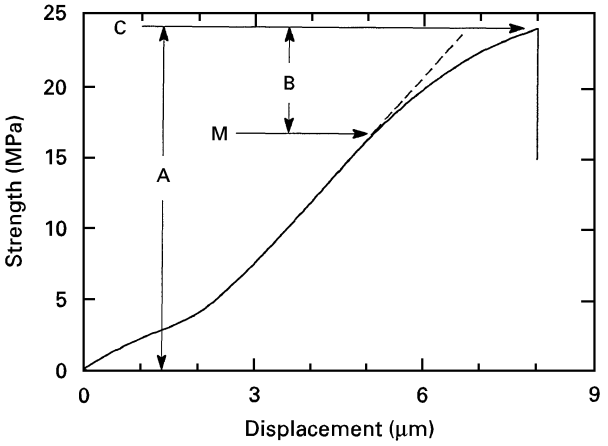

Figure 3 Displacement–strength curve.

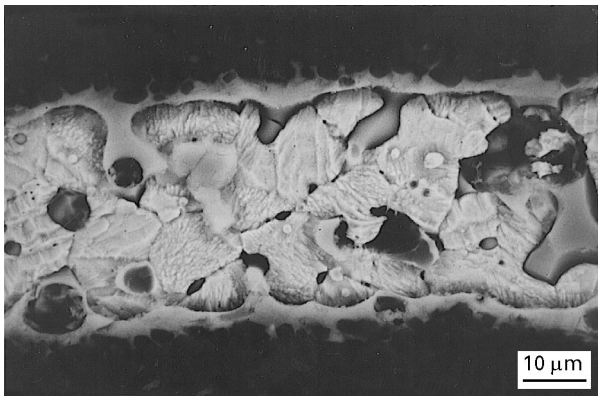

Figure 4 A typical microstructure of a silver thick-film.

decrease at point M was caused by the thickness change of the thick film. No crack was observed in the cross-section of a specimen that was unloaded before point M. On the other hand, some cracks were observed in the cross-section of a specimen that was unloaded between points M and C. These facts indicate that the crack initiated at point M. The formation and propagation of the crack parallel to the substrates increased the apparent thickness of the thick film. As a result, the gradient of the displacement–strength curve decreased.

At point M, the thick film did not fracture completely. This means that the crack propagated very slowly or stopped between points M and C. Therefore, B denotes the stress under the influence of crack. Results of acoustic emission (AE) spectroscopic analysis supported the above view. High amplitude signals of AE events appeared at the displacement corresponding to point M in Fig. 3.

At point C, the thick film fractured completely. Thus, A denotes the adhesion strength. We defined the percentage of B to A as the percentage of stress (PS), which is related to the resistance to crack propagation. Point M was defined as the point at which the curve deviated from the straight line by more than 5% (cf., Fig. 3). When the displacement was too small, point M was not detected, which corresponds to a PS of 0%. So, the calculated PS can be lower than the real value.

3.2. Microstructure development and crack site

Fig. 4 illustrates a typical cross-section of an etched thick film. Dark-coloured areas at both sides of the silver-layer are substrates, grey areas are glass, light-coloured areas are silver, and black areas in silver are pores. The thick film consists of two glass layers in contact with the substrates and a silver layer that contains glass and pores. Glass softened and penetrated into grain boundaries of silver particles during firing. The silver particles rearranged and the grain growth occurred by the solution–precipitation mechanism. Glass was squeezed from the silver partiles, moved to the silver–substrate interfaces, and penetrated into the grain boundaries of the substrates [13].

Cracks of various types in thick films are illustrated in Fig. 5, which were obtained by releasing the load between points M and C in Fig. 3. Fig. 5a and b illustrates cracks that propagated parallel to the substrates through the glass layers and glass–silver interfaces from right to left, respectively. Fig. 5a shows that the crack through the glass layer was deflected at the glass–silver interface and then propagated along the glass–silver interface. Crack deflection at the glass–substrate interface was also observed in other specimens. The probability of crack deflection at the glass–silver and glass–substrate interfaces was high in specimens with thin glass layers. Fig. 5b illustrates a crack that propagated along the glass–silver interface and then deflected to the glass layer. Fig. 5c illustrates a crack that propagated through the silver layer vertically to the substrates. Fracture of the silver layer involved pores and the glass phase. Another important feature is that fracture at the glass–substrate interface was not observed. Hence, strong bonding between the glass layer and the substrate is expected.

3.3. Adhesion strength and microstructure

In order to study the microstructure–property relations, three parameters were introduced to characterize the microstructure: porosity of the silver layer, thickness of the glass layer, and roughness of the glass–silver interface. Table II lists the microstructural parameters of thick films prepared under various conditions. Here, data for specimen Bm7 were taken as a reference for comparison. The microstructure of silver thick films is known to depend on the softening point of glass relative to the densification temperature of silver powders, the firing temperature and the glass content [14, 15]. When the softening point is lower than the densification temperature of silver particles, softening of glass enhances the rearrangement of silver particles, resulting in dense thick films. Specimen Am7 corresponds to this case. On the other hand, when the softening point is higher than the densification temperature of silver particles, softening of glass does not enhance rearrangement of silver particles, resulting in

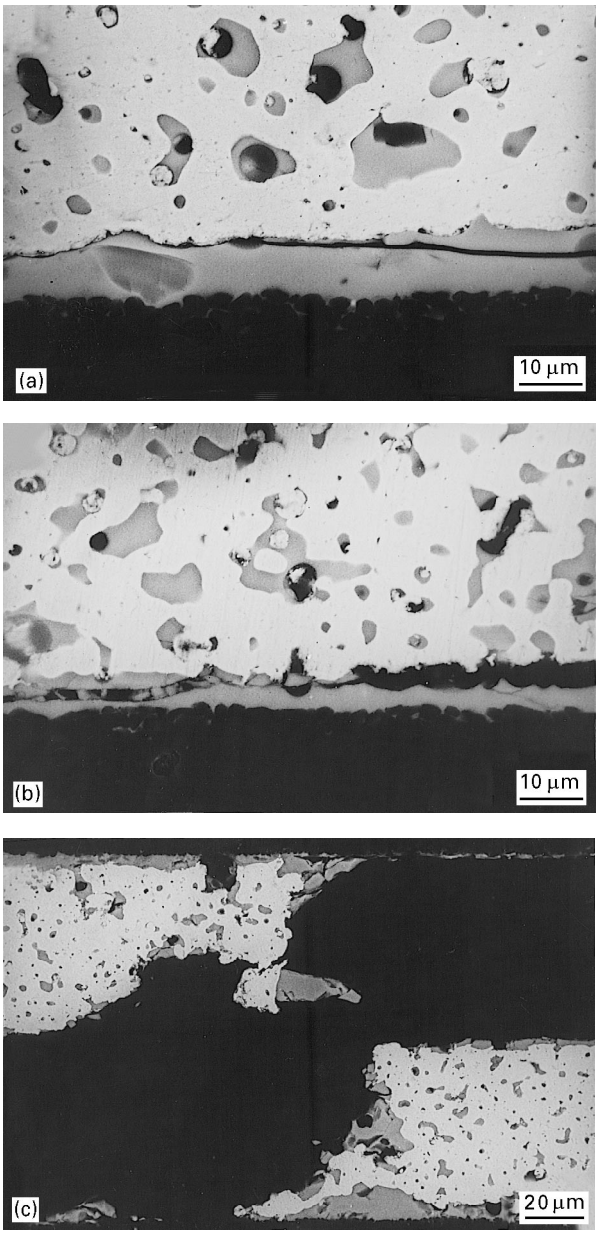

Figure 5 Cracks in silver thick-films obtained by releasing the load between the points M and C in Fig. 3: (a) crack through glass layer to glass–silver interface parallel to the substrate, (b) crack through glass–silver interface to glass layer parallel to the substrate, and (c) crack through silver layer vertical to the substrate.

porous thick films like Cm7. At high firing temperatures, densification of the silver layer is accelerated and glass is pushed out from the silver layer resulting in thick glass layers. The glass–silver interface becomes smoother with densification of the silver layer. The glass content affects the thickness of the glass layer and the porosity of the silver layer. For instance, the higher glass content results in thicker glass layers. In thick films with low glass contents, the porosity in the silver layer is high. Based on the above discussion, adhesion strength will be discussed in correlation with the microstructure.

Table II shows that specimens with high PS, such as B17, B117 and Bm7f, have high adhesion strengths. In other words, higher resistance to crack propagation can give higher adhesion strength. High PS specimens showed thin glass layers or rough glass–silver interfaces. A crack is difficult to propagate through a thin glass layer or a rough interface. Thus, specimens with thin glass layers and rough interfaces should give high adhesion strengths. However, Cm7 and Bm6 with thin glass layers showed low adhesion strengths. In these specimens, discontinuous glass layers were formed, because glass did not fully wet the silver layer due to the low viscosity of the glass at the firing temperature. Table II also shows that specimens with low PS, such as Am7, Bm8, Bm7 and Cm7, have low or medium adhesion strengths. In other words, lower resistance to crack propagation leads to lower adhesion strengths. Specimens with thick glass layers or smooth glass–silver interfaces gave low PS. A crack is easy to propagate along the thick glass layer or a smooth interface. Therefore, high adhesion strengths cannot be expected from specimens with a thick glass layer or smooth interface.

The porosity of the silver layer has not been well correlated with PS, though porous thick films showed low adhesion strengths in most cases. Therefore, crack propagation behaviour was studied by observing cross-sections of partially loaded specimens, which were obtained by releasing the load between points M and C in the strength–displacement curve shown in Fig. 3. Examination of variously processed thick films revealed that the fracture occurred catastrophically in

TABLE II Strength, PS and microstructure

Specimen[a]	Adhesion strength (MPa)	PS (%)	Microstructure		
			Porosity of Ag layer	Thickness of glass layer	Roughness of glass–Ag interface
Am7	17.8	1.82	Low	Thick	Medium
Bm7	17.6	7.87	Medium	Medium	Medium
Cm7	9.5	5.79	High	Thin	Rough
Bm6	16.2	5.88	High	Thin	Medium
Bm8	19.8	2.61	Low	Medium	Smooth
Bll7	20.3	9.18	High	Thin	Medium
Bl7	23.9	10.59	Medium	Thin	Medium
Bh7	12.2	2.28	Medium	Thick	Medium
Bm7f	23.9	8.87	Low	Thin	Rough

[a] See Table I for specimens.

the silver layer. Fig. 6 illustrates a typical example. Two cracks propagated through the glass layers on both sides of the silver layer in opposite directions; the right-hand side of the thick film was pulled and the left-hand side was pushed. Thus, a shear stress vertical to the substrate is developed, causing the thick film to fracture. Microscopic observation also revealed that fracture in the silver layer occurred vertically, not parallel to the substrate. Poor dependence of PS on the porosity of the silver layer can be explained by the fracture behaviour just described.

Table II shows that porous thick films have low adhesion strength, except for Bll7. In most cases, high porosity implies poor bonding of silver grains, which leads to low adhesion strength. The relatively high adhesion strength of specimen Bll7 can be explained by the low glass content. Summarizing the above discussion, we propose microstructural requirements for designing thick films with high adhesion strength. They are thin layer, rough glass–silver interface and low porosity.

Next, we tested the applicability of distribution functions to the adhesion strength of thick films. Table III lists the correlation coefficients of the adhesion strengths to the straight lines on the Weibull, normal and log-normal probability papers. The log-normal distribution function gave high correlation for most preparation conditions. Weibull [16] and normal distribution functions often apply to the tensile strength of brittle and ductile fracture, respectively. The thick film conductor is a composite of ductile and brittle materials. The adhesion strength of silver thick films has not been adequately described by Weibull or normal distribution functions.

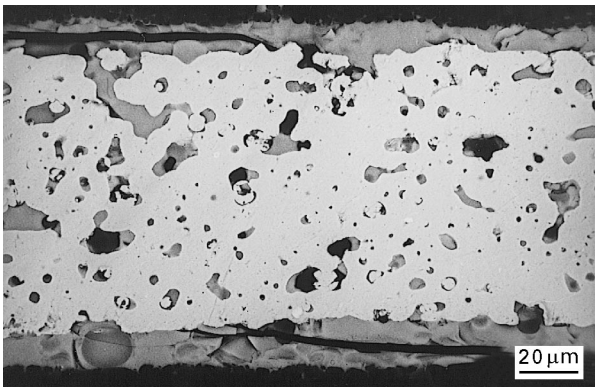

Figure 6 Two cracks that propagated through the glass layer in opposite directions.

TABLE III Correlation coefficient of distributions for adhesion strength of thick-films

Specimen[a]	Weibull distribution	Normal distribution	Log-normal distribution
Am7	0.983	0.972	0.986
Bm7	0.969	0.870	0.989
Cm7	0.949	0.958	0.976
Bm6	0.954	0.984	0.896
Bm8	0.972	0.959	0.986
Bll7	0.974	0.974	0.991
Bl7	0.974	0.982	0.983
Bh7	0.992	0.974	0.986
Bm7f	0.948	0.960	0.981

[a] See Table I for specimens.

4. Conclusions

The adhesion strength of silver thick films was evaluated by a new solder-free test. A parameter PS (percentage of stress), a measure for the resistance to crack propagation, was introduced to study the relation between microstructure and adhesion strength more precisely. Thick films with a thin glass layer or rough glass–silver interface gave high PS. Low porosity silver layers, a thin glass layer and a rough glass–silver interface were essential for high adhesion strengths. The log-normal distribution function best described the adhesion strength of silver thick films.

Acknowledgement

The authors gratefully thank TDK Corporation for assistance in various fields in executing this work.

References

1. "The thick film handbook" (Photo Products Department E.I. DuPont De Nemours & Co., Inc., Wilmington, DE, 1971).
2. C. R. N. NEEDS and J. P. BROWN, in Proceedings of the International Symposium on Microelectronics, October 1989 (ISHM, Reston, VA, 1989) p. 211.
3. T. T. HITCH, in Proceedings of the International Symposium on Microelectronics, November 1985 (ISHM, Reston, VA, 1985) p. 529.
4. Y. KURIHARA, S. TAKAHASHI, K. YAMADA and T. ENDO, *IEEE Trans. Comp. Hybrids Manuf. Technol.* **CHMT-13** (1990) 306.
5. B. CHIOU, K. C. LIU, J. DUH and P. S. PALANISAMY, *ibid.* **CHMT-13** (1990) 267.
6. P. J. WHALEN and J. B. BLUM, *ibid.* **CHMT-9** (1986) 161.
7. *Idem*; *ibid.* **CHMT-9** (1986) 168.
8. N. TANIFUJI and Y. MORIMOTO, in Proceedings of the International Symposium on Microelectronics, October 1989 (ISHM, Reston, VA, 1989) p. 313.
9. J. MURAYAMA, H. IKEZAKI, N. TANIFUJI and T. KATO, *ibid.* p. 303.
10. H. G. KIM, W. ROTHLINGSHOFER and G. TOMANDL, *Solid State Technol.* **22** (1979) 62.
11. W. D. BASCOM and J. L. BITNER, *J. Mater. Sci.* **12** (1977) 1401.
12. P. F. BECHER and W. L. NEWELL, *ibid.* **12** (1977) 90.
13. M. E. TWENTYMAN, *ibid.* **10** (1975) 765.
14. T. YAMAGUCHI and H. IMAI, *Ceram. Trans.* **15** (1990) 347.
15. K. YATA, Y. ENOKIDO and T. YAMAGUCHI, *IEEE Trans. Comp. Hybrids Manuf. Technol.* **CHMT-16** (1993) 584.
16. W. WEIBULL, *J. Appl. Mec.* **18** (1951) 293.

Received 1 November 1995
and accepted 10 February 1997